TOXICOLOGICAL SCIENCES, 163(1), 2018, 279–292

doi: 10.1093/toxsci/kfy038
Advance Access Publication Date: February 15, 2018
Research Article

Multidrug Resistance Protein 1 Deficiency Promotes Doxorubicin-Induced Ovarian Toxicity in Female Mice

Yingzheng Wang,* Mingjun Liu,* Jiyang Zhang,† Yuwen Liu,‡ Megan Kopp,* Weiwei Zheng,§ and Shuo Xiao*,[1]

*Department of Environmental Health Sciences, Arnold School of Public Health, University of South Carolina, Columbia, South Carolina 29208; †Department of Obstetrics and Gynecology, Feinberg School of Medicine, Northwestern University, Chicago, Illinois 60611; ‡Department of Human Genetics, The University of Chicago, Chicago, Illinois 60637; and §Key Laboratory of Public Health Safety, Ministry of Education, Department of Environmental Health, School of Public Health, Institution for Water Pollution and Health Research, Fudan University, Shanghai 20032, China

[1]To whom correspondence should be addressed at Department of Environmental Health Sciences, Arnold School of Public Health, University of South Carolina, 915 Greene Street, Room 327, Columbia, SC 29208. Tel: 803-777-6745; Fax: 803-777-3391; E-mail: sxiao@mailbox.sc.edu.

ABSTRACT

Multidrug resistance protein 1 (MDR1), a phase III drug transporter that exports substrates out of cells, has been discovered in both cancerous and normal tissues. The over expression of MDR1 in cancer cells contributes to multiple drug resistance, whereas the MDR1 in normal tissues protects them from chemical-induced toxicity. Currently, the role of MDR1 in the ovary has not been entirely understood. Our objective is to determine the function of MDR1 in protecting against chemotherapy-induced ovarian toxicity. Using both the *in vivo* transgenic mouse model and *in vitro* follicle culture model, we investigated the expression of MDR1 in the ovary, the effect of MDR1 deficiency on doxorubicin (DOX)-induced ovarian toxicity, and the ovarian steroid hormonal regulation of MDR1. Results showed that the MDR1 was expressed in the ovarian epithelial cells, stroma cells, theca cell layers, endothelial cells, and luteal cells. The lack of MDR1 did not affect female ovarian function and fertility; however, its deficiency significantly exacerbated the DOX-induced ovarian toxicity in both *in vivo* and *in vitro* models. The MDR1 showed significantly higher expression levels in the ovaries at estrus and metestrus stages than those at proestrus and diestrus stages. However, this dynamic expression pattern was not regulated by the ovarian steroid hormones of estrogen (E2) and progesterone (P4) but correlated to the number and status of corpus luteum. In conclusion, our study demonstrates that the lack of MDR1 promotes DOX-induced ovarian toxicity, suggesting the critical role of MDR1 in protecting female ovarian functions during chemotherapy.

Key words: MDR1; doxorubicin; follicle; chemotherapy; ovarian toxicity.

With the significantly improved cancer survival rates in the past several decades, there is now an increased awareness regarding the side effects from anticancer treatments in nontumorous organs (Chabner and Roberts, 2005). The ovary is the primary female reproductive organ and functions to support hormone secretion and germ cell-oocyte maturation. Ovarian toxicity resulting from chemotherapy is one of the major concerns for young female cancer patients (Morgan *et al.*, 2012). To date, multiple chemotherapeutic chemicals have been demonstrated to damage ovarian follicles and increase the risk of sub- or in-fertility (Bines *et al.*, 1996; Morgan *et al.*, 2012).

Multidrug resistance protein 1 (MDR1), also known as ATP-binding cassette transporter B1 (ABCB1) or P-glycoprotein, is a phase III drug transporter that exports substrates out of cells by using energy from ATP hydrolysis (Gottesman and Pastan, 1988). Humans have one type of MDR1, whereas mice have 2 isoforms, MDR1a and MDR1b. MDR1 was first identified in cancer cells, and its overexpression contributes to anticancer drug

resistance by extruding drugs out of tumorous cells (Borst and Schinkel, 2013; Kartner *et al.*, 1985; Riordan *et al.*, 1985). MDR1 is also expressed in the cells of normal tissues including the blood-brain barrier, liver, small intestine, and kidney (Cordon-cardo *et al.*, 1989; Schinkel *et al.*, 1994), and functions to restrict xenobiotic accumulation in these tissues and thereby protecting them from the chemical-induced toxicity. For example, MDR1a is the main isoform in the blood-brain barrier and mice with an absence of *Mdr1a* had increased brain accumulation of vinblastine (a chemo-drug for breast and testicle cancer, etc.) and were 100-fold more sensitive to the vinblastine-induced neurotoxicity than the wild type (WT) littermates (Schinkel *et al.*, 1994). Currently, multiple MDR1 inhibitors are actively investigated to overcome the MDR1-mediated multiple drug resistance in tumor cells (Abraham *et al.*, 2009; Dantzig *et al.*, 1996; Kolitz *et al.*, 2010). However, the inhibition of MDR1 potentially increases the side effects of chemotherapeutic chemicals in nontumorous tissues.

In the female reproductive system, studies have reported that MDR1 was highly expressed in the pregnant rodent uterine endometrium, vascular endothelial cells, and placenta, and mice lacking MDR1 had increased placental penetration of avermectin (a drug for treating parasitic worms) and the avermectin-induced teratogenicity (Arceci *et al.*, 1988; Huang *et al.*, 2016; Kalabis *et al.*, 2005; Lankas *et al.*, 1998), suggesting the critical role of MDR1 in protecting fetuses from teratogens during pregnancy. In the ovary, MDR1 has been found in human ovarian epithelium, theca cells, luteal cells, and endothelial cells (Finstad *et al.*, 1990); and others have reported that MDR1 was also expressed in the porcine and mouse granulosa cells and oocytes (Arai *et al.*, 2006; Brayboy *et al.*, 2013, 2017; Fukuda *et al.*, 2006). The function of MDR1 expressed in the ovary is still poorly understood. Arai *et al.* (2006) found that the porcine oocytes exhibited MDR1-mediated efflux activity and oocytes in metaphase II (MII) stage had stronger exporting activity than oocytes in the germinal vesicle (GV) stage. However, in human oocytes, another group revealed that GV oocytes were more efficient for the MDR1-mediated efflux than MII oocytes, and the inhibition of MDR1 significantly increased the cyclophosphamide-induced oocyte death (Brayboy *et al.*, 2017). Using *in vitro* cultured granulosa cell lines (KK15 immortalized murine granulosa cells), Salih *et al.* reported that the over expression of MDR1 inhibited the chemotherapy-induced cytotoxicity (Salih, 2011). These results indicate that MDR1 may play important roles in protecting the ovary from chemotherapy-induced toxicity. However, these studies have relied on *in vitro* cultured granulosa cells or denuded oocytes without surrounding somatic cells, which do not represent the exposure pattern of the intact ovary or ovarian follicles during chemotherapy. Using a transgenic animal model, Brayboy *et al.* (2017) reported that mice lacking both MDR1 and breast cancer resistance protein (BCRP) had significantly increased ovarian cell death upon cyclophosphamide exposure, but the deletion of both MDR1 and BCRP is unable to differentiate whether the exacerbated ovarian toxicity is caused by the absence of MDR1 and/or by the absence of BCRP.

Doxorubicin (DOX), one of the most commonly used anticancer medications, is a validated MDR1 substrate and has been widely used to study the role of MDR1 in inducing multiple drug resistance in cancerous cells as well as in protecting chemical-induced toxicity in non-tumorous tissues (Dantzig *et al.*, 1996; Luker *et al.*, 2001). Our group and others have demonstrated that DOX damaged mitotically active granulosa cells, induced follicle apoptosis, and ultimately disturbed female ovarian function and fertility (Bar-Joseph *et al.*, 2010; Ben-Aharon *et al.*, 2010; Kropp *et al.*, 2015; Perez *et al.*, 1997; Roti Roti *et al.*, 2012; Xiao *et al.*, 2017). Therefore, using both *in vivo* transgenic mouse model and *in vitro* follicle culture model, the present study is aimed to determine the function of MDR1 in protecting against DOX-induced ovarian toxicity. This study is critical because the MDR1 inhibitors are being tested to promote the anticancer drug efficacy and human MDR1 genetic variants have also been discovered to affect MDR1 efflux activity (Leschziner *et al.*, 2007), both of which potentially increase the risk of female ovarian dysfunction and infertility during chemotherapy.

MATERIALS AND METHODS

Animals. Both WT and *Mdr1a/b*$^{-/-}$ male and female breeders were purchased from Taconic (Taconic, Hudson, NY) which were generated from the FVB/N mouse strain. The mouse breeding colony was maintained in the animal facilities of Northwestern University (NU) and University of South Carolina (USC). All mice were housed in polypropylene cages and provided food and water ad libitum. The animals were kept on a 12-h light/dark cycle (7:00 AM to 7:00 PM) at 23°C ± 1°C with 30%-50% relative humidity. Animals were fed Teklad Global irradiated 2919 or 2916 chow (Madison, WI), which does not contain soybean or alfalfa meal to minimize the exposure to phytoestrogens. All methods used in this study were approved by Institutional Animal Care and Use Committee (IACUC) in NU and USC and correspond to the National Institutes of Health guidelines and public laws. All the animal related experiments were performed in NU except the individual follicle and ovarian explants isolation, culture, and hormone treatment, so the potential influence of animal facility on experimental results could be excluded.

Reverse transcription-qPCR. The expression of *Mdr1a* and *Mdr1b* in different female reproductive organs, were examined by quantitative reverse transcription PCR (RT-qPCR) as previously described in Xiao *et al.* (2017). Five adult mice at estrus stage were used to avoid the potential influence of ovarian cyclicity on the MDR1 expression in the ovary. Moreover, the expression of *Mdr1a* and *Mdr1b* in the ovaries at different stages of estrous cycle and in ovarian explants upon different concentrations of hormone treatment was also quantified by RT-qPCR, with 3-5 mice for each estrous cycle stage and 4 ovarian explants for each hormonal treatment group. Total RNA was extracted using Trizol (Invitrogen, Carlsbad, CA). cDNA was reverse-transcribed from 1 μg of total RNA using Superscript III reverse transcriptase with random primers (Invitrogen, Carlsbad, California). qPCR was performed in 96-well or 384-well plates using SYBR-Green I intercalating dye on ABI 7900 (Applied Biosystems, Carlsbad, CA). qPCR thermos cycle was programmed for 30 s (s) at 95°C, followed by 35 cycles of 30 s at 95°C and 30 s at 56°C, and ended with 30 s at 72°C and 5 min at 72°C. The mRNA expression levels of *Mdr1a* and *Mdr1b* were normalized by the expression of house-keeping gene- *Gapdh (glyceraldehyde-3-phosphate dehydrogenase)* to indicate the relative gene expression levels. Primers were designed and the sequences were (Integrated DNA Technologies, Coralville, IA): *Mdr1a* forward: tggactgtcagctggtattt, *Mdr1a* reversed: caatatttggagatgcctgt; *Mdr1b* forward: atccc aagatccttttgttg, *Mdr1b* reversed: tgctttctgtggacacttct; *Gapdh* forward: gccgagaatgggaagcttgtcat, *Gapdh* reversed: gtggttcacacccatc acaaacat.

Histology, immunohistochemistry, and immunofluorescence. The ovary, oviduct and uterus were collected from 3 to 5 prepubertal (days 22–26 before vaginal opening) and 5 adult (8 weeks of age) female mice and fixed in 10% formalin at 4°C overnight, embedded in paraffin, and sectioned at the thickness of 5 μm. Ovarian sections were stained with hematoxylin and eosin (H&E) at every fifth section for histology as previously described in Xiao *et al*, (2015). The expression of MDR1 in different female reproductive organs and in ovaries at different stages of estrous cycle was determined by immunohistochemistry (IHC). Briefly, after deparaffinization and rehydration, ovarian sections underwent antigen retrieval in the freshly made sodium citrate buffer (10 mM sodium citrate and 0.05% Tween-20, pH 6.0, ThermoFisher Scientific, Grand Island, NY) in a pressure cooker for 40 min. After being washed 3 times in phosphate-buffered saline (PBS) for 5 min each, slides were incubated with 3% hydrogen peroxide in Tris-buffered saline for 15 min. Nonspecific binding was then blocked with 1% bovine serum albumin (BSA, Sigma-Aldrich, St Louis, MO) for 1 h which was followed by incubating with the primary rabbit antiMDR1 antibody (1:200, ab170904, Abcam, Cambridge, MA) in blocking solution at 4°C overnight. On the second day, ovarian sections were washed 3 times in PBS for 5 min each, incubated with HRP conjugated goat antirabbit secondary antibody (1:500, ab6721, Abcam, Cambridge, MA) in blocking solution for 1 h at room temperature (RT), and washed in PBS twice for 5 min each. The PBS washed sections were then stained with DAB substrate kit (ab64238, Abcam, Cambridge, MA), counterstained with hematoxylin, and mounted for imaging. MDR1 has been reported to express in the renal tubule cells; we thus use the kidney as positive control (Thiebaut *et al*., 1987). The dual staining of MDR1 and α-smooth muscle actin (α-SMA, marker for smooth muscle cells) was performed by immunofluorescence (IF). The protocol on day 1 was the same as IHC except that the antiα-SMA antibody (1:200, ab7817, Abcam, Cambridge, MA) was also added. On the second day, ovarian sections were washed 3 times in PBS for 5 min each, incubated with Alexa Fluor 488 goat antirabbit IgG and Alexa Fluor 568 rabbit antimouse IgG (1:200, Life Technology, Grand Island, NY) in blocking solution for 1 h at RT, and washed in PBS twice for 5 min each. The ovarian sections were mounted in Vectashield containing 4', 6-diamidino-2-phenylindole (DAPI, Vector Laboratory, Burlingame, CA). Ovarian sections for negative control were processed with the same procedures, except that the primary antibody was replaced with goat antirabbit IgG and goat antimouse IgG (1:200, Abcam, Cambridge, MA). Signals for IHC and IF were visualized using an EVOS FL AUTO microscope (Life Technology, Grand Island, NY).

Female mouse superovulation and fertility test. To determine whether the lack of MDR1 affects ovarian follicle development and oocyte maturation, superovulation was performed in both 8-week-old WT and *Mdr1a/b*$^{-/-}$ female mice by intraperitoneal injection of 5 IU of pregnant mare's serum gonadotropin (PMSG) (Sigma-Aldrich, St Louis, MO), followed by a 5 IU of human chorionic gonadotropin (hCG, Sigma-Aldrich, St Louis, MO) 48 h after the PMSG injection. Oocytes were collected from the ampulla of the oviduct 14 h after the hCG injection and were denuded from surrounding cumulus cells using 0.3% hyaluronidase (Sigma-Aldrich, St Louis, MO). The total number of ovulated oocytes and the number of oocytes with polar body extrusion (MII oocytes) were counted. For the mouse fertility test, both 8-week-old virgin WT and *Mdr1a/b*$^{-/-}$ female mice were naturally mated with proven fertile WT males with 2 females and 1 male per cage. Once the mating was established with the presence of vaginal plug, females were separated from males and were housed individually until delivery. Upon delivery, gestation period, litter size, gender, and number of live and dead pups were recorded. The female mice were kept with their pups for 21 days until the pups were weaned and then the adult females were mated with proven fertile males again. For superovulation study, 4–6 female mice were included for each replicate and 3 replicates were performed. For the fertility test, 4 female mice were included for each genotype and 4 mating rounds were completed.

DOX exposure in vivo, superovulation, and TUNEL assay. In humans, the DOX treatment dosage ranges from 8 to 400 mg/m^2, which are equivalent to 0–10 mg/kg. We have previously demonstrated that DOX has dose-dependent ovarian toxicity and 2–10 mg/kg of DOX significantly disrupts the oocyte reproductive outcomes (Xiao *et al*., 2017). To determine whether the lack of MDR1 affects the susceptibility of mice toward DOX-induced ovarian toxicity, 22-day-old WT and *Mdr1a/b*$^{-/-}$ female mice were intraperitoneally injected once with 0, 0.4, and 2 mg/kg of DOX (Sigma-Aldrich, St Louis, MO) dissolved in 100 μl dimethyl sulfoxide (DMSO, Sigma-Aldrich) or with 100 μl DMSO only as control. The prepubertal mice were selected because we demonstrated that the MDR1 had different expression levels at different stage of estrous cycle (Fig. 7). Half of DOX-treated mice were sacrificed 24 h after injection. One side of ovaries were snap frozen for cleaved caspase 3 (C-CASP3) measurement and the other side of ovaries were fixed, embedded, and sectioned as described earlier. Ovarian cell apoptosis was determined by terminal deoxynucleotidyl transferase 2'-Deoxyuridine, 5'-Triphosphate nick end labeling (TUNEL) assay using the DeadEnd Fluorometric TUNEL System (Promega, Madison, MI) following manufacturer's instructions, and the incubation buffer without rTdT enzyme was used as the negative control. The other half of mice underwent superovulation with PMSG and hCG injections and oocytes were collected on day 8 post DOX/vehicle injection, respectively, and the total number of ovulated oocytes and the percentage of MII oocytes were calculated. For the *in vivo* DOX exposure experiment, 4–6 mice were included in each phenotype and dose group. For TUNEL staining, 5 ovarian sections for each ovary were included.

C-CASP3 measurement. The whole ovary C-CASP3 levels were quantified using Mouse Active caspase-3 ELISA kit (MBS7210856, MyBioSource, San Diego, CA). Ovaries from both WT and *Mdr1a/b*$^{-/-}$ mice with different concentrations of DOX exposure were collected as described earlier, rinsed in ice-cold PBS briefly, weighted, and homogenized in 500 μl of PBS on ice. The homogenates were centrifuged for 15 min at 5000 rpm and the supernatant was used for ELISA according to manufacturer's instruction. All samples and standards were run in duplicate and the intensity of color was measured spectrophotometrically at 450 nm in a microplate reader (BioTek, Winooski, VT).

Rhodamine 123 incubation assay. Rhodamine 123 (Rho123) is a validated MDR1 transported fluorescent dye (Forster *et al*., 2012), and due to the positive correlation between the MDR1-mediated efflux activity and the cellular Rho123 green fluorescent staining, the Rho123 incubation assay is a valuable tool to determine the MDR1-mediated efflux activity (Altenberg *et al*., 1994; Lee *et al*., 1994). Multilayered secondary follicles with diameter between 150 and 180 μm were mechanically isolated from 16-day-old CD-1 female mice as previously described (Xiao *et al*., 2015, 2017). Only follicles with intact theca cell layers and attached stroma cells were selected. The isolated follicles were placed in

growth media containing α minimal essential medium (αMEM) Glutamax supplemented with 3 mg/ml BSA (Sigma-Aldrich, St Louis, MO), 10 mIU/ml recombinant follicle-stimulating hormone (from A. F. Parlow, National Hormone and Peptide Program, National Institute of Diabetes and Digestive and Kidney Diseases, Bethesda, MD), 1 mg/ml bovine fetuin (Sigma-Aldrich, St Louis, MO), 5 μg/ml insulin, 5 μg/ml transferrin, and 5 μg/ml selenium (Sigma-Aldrich, St Louis, MO). Follicles were randomly distributed into 2 groups and pre-incubated with 0 and 1 μM of MDR1 inhibitor PSC833 (Abcam, St Louis, MO) in the growth media for 30 mins at 37°C in 5% CO_2, respectively. The concentration of PSC833 was selected based on previous studies which have demonstrated to effectively inhibit the MDR1-mediated efflux activity (Altenberg *et al.*, 1994; Lee *et al.*, 1994). Follicles were then treated with 1 μg/ml of Rho123 (ThermoFisher Scientific, Grand Island, NY) in the growth media with and without PSC833 for 30 min at 37°C in 5% CO_2. The Rho123 green fluorescence was imaged using EVOS FL AUTO microscope at 0, 10, 20, and 30 min and the fluorescent intensity was analyzed using ImageJ (National Institutes of Health, Bethesda, MD). For both control and PSC833 treatment groups, 13–20 follicles for each replicate and 3 replicates were performed.

In vitro *follicle encapsulation, culture, and DOX exposure*. Multilayered secondary follicles with diameter between 150 and 180 μm from day-16-old WT and *Mdr1a/b*$^{-/-}$ female mice were isolated as previously described (Xiao *et al.*, 2015, 2017). Similar to the MDR1 efflux activity test, only follicles which displayed intact theca cell layers and with attached stroma cells were selected. Briefly, follicles were placed in the maintenance media containing 50% αMEM (Glutamax) and 50% Nutrient Mixture (F-12 with Glutamax) with 1% fetal bovine serum (Life Technology, Grand Island, NY) for 2 h before encapsulation. Follicles were then encapsulated individually in 0.5% alginate (NovaMatrix, Sandvika, Norway) as previously described (Xiao *et al.*, 2015, 2017). Alginate beads were placed individually in 96-well plates, with each well containing 100 μl growth media. For all experiments, follicles were maintained at 37°C. The plasma concentration of DOX for human who received chemotherapy ranges from 2 to 100 nM (Speth *et al.*, 1988; Sturgill *et al.*, 2000). Therefore, follicles were exposed to DOX at human relevant concentrations of 0, 1, 10, and 100 nM on day 0 for 24 h. Follicles were then washed 3 times for 15 min each with growth media to remove the remaining DOX and were continued in culture for up to 8 days. Half of the growth media (50 μl) was replaced every other day. Follicles were imaged at each media change using an inverted Leica DM IRB microscope with 4× and 20× objectives (Leica Microsystems, Buffalo Grove, IL). Follicle diameter was calculated by averaging 2 perpendicular measurements from basement membrane to basement membrane of each follicle in ImageJ software (National Institutes of Health, Bethesda, MD). For each phenotype and DOX exposure group, 12–15 follicles for each replicate and 3 replicates of encapsulated *in vitro* follicle growth (eIVFG) were performed. Follicles were considered dead if they had unhealthy appearing oocytes and/or granulosa cells, or if the integrity of the oocyte and somatic cell interface was visibly compromised. The follicle growth curves and survival rates on days 0, 2, 4, 6, and 8 were plotted and the lethal concentration 50 (LC50) with 90% CI of DOX on *in vitro* cultured follicles was calculated.

Ovarian cyclicity assessment, corpus luteum count, and experiments of ovarian steroid hormonal regulation of MDR1. To determine the effect of ovarian estrous cycle and steroid hormones on the expression of *Mdr1a* and *Mdr1b*, ovarian cyclicity for adult female mice was assessed by performing daily vaginal smears between 1500 and 1600 h every day and examining the morphology of vaginal epithelial cells and the presence of leucocytes to determine the estrous cycle stage as previously described (Byers *et al.*, 2012; Zhao *et al.*, 2013). WT female mice with different stages of estrous cycle were sacrificed. One side of ovaries from each mouse was used for RNA extraction and RT-qPCR. The other side of ovaries were fixed, embedded, and sectioned as described above. Ovarian sections were stained with H&E at every fifth section for histology and the number of corpus luteum (CL) was counted and the counts were normalized to the entire ovary. Since the CL can persist across multiple stages of estrous cycle(s) and 1 ovary can contain different developmental status of CLs, we classified the CL into 3 stages: (1) The newly formed CL that was characterized by the small basophilic cells which are morphologically similar to the granulosa cells; (2) the mature CL that was characterized by the plump cell shape and moderate amounts of eosinophilic cytoplasm; and (3) the degenerated CL that was characterized by presence of vacuoles and luteal cell debris (Stocco *et al.*, 2007). The nonH&E stained sections were selected to perform the IHC for MDR1 staining as described earlier.

To further investigate the hormonal regulation of MDR1, serum was also collected and the E2 and P4 concentrations were measured using ELISA kits (Calbiotech, Spring Valley, CA). The mRNA expression of *Mdr1a* and *Mdr1b* in the ovary was correlated to the corresponding levels of serum E2 and P4, respectively, for each mouse. Moreover, the ovaries without CL were collected from prepubertal 16-day-old mice; and the ovaries with CL were collected from superovulated 26-day-old mice treated with PMSG and hCG on 23 and 25 of days of age, respectively. The presence of clusters cumulus-oocyte-complex in the ampulla region of oviduct was used to confirm the successful superovulation induction. Each ovary was cut into 4 even pieces within the dissection medium and 2 quarters of ovarian pieces were placed on a 0.4 μm cell culture insert (EMD Millipore, Burlington, MA) in the 24-well tissue culture plate, with each well containing 500 μl growth media. The ovarian explants were treated with E2 at 0, 1, and 10 pg/ml and with P4 at 0, 1, and 10 ng/ml for 6 h, respectively. Ovarian explants were then collected for total RNA extraction and RT-qPCR to examine the expression of *Mdr1a* and *Mdr1b*.

Statistical analyses. The MDR1 gene expression levels, total oocyte number, litter size, Rho 123 fluorescent intensity, C-CASP3 levels, follicle growth, and survival were analyzed using Repeated Measures ANOVA. Categorized data of the MII oocyte percentage were analyzed by the Kruskal-Wallis H test, and the post hoc test was performed to compare the difference between 2 groups if the significant difference was observed. The correlation between the mRNA levels of *Mdr1a* and *Mdr1b* and the serum levels of E2, P4, and P4/E2 was analyzed by linear regression method and the coefficient of determination (R^2) were calculated. The significance level was set at $p < .05$.

RESULTS

Expression of MDR1 in the Mouse Female Reproductive System

RT-qPCR and IHC were performed to determine the expression of MDR1 in different female reproductive organs. All tissues were collected from adult female mice at estrus stage. RT-qPCR revealed that *Mdr1a* had significantly higher expression levels in the uterus than that in the ovary and oviduct, whereas *Mdr1b*

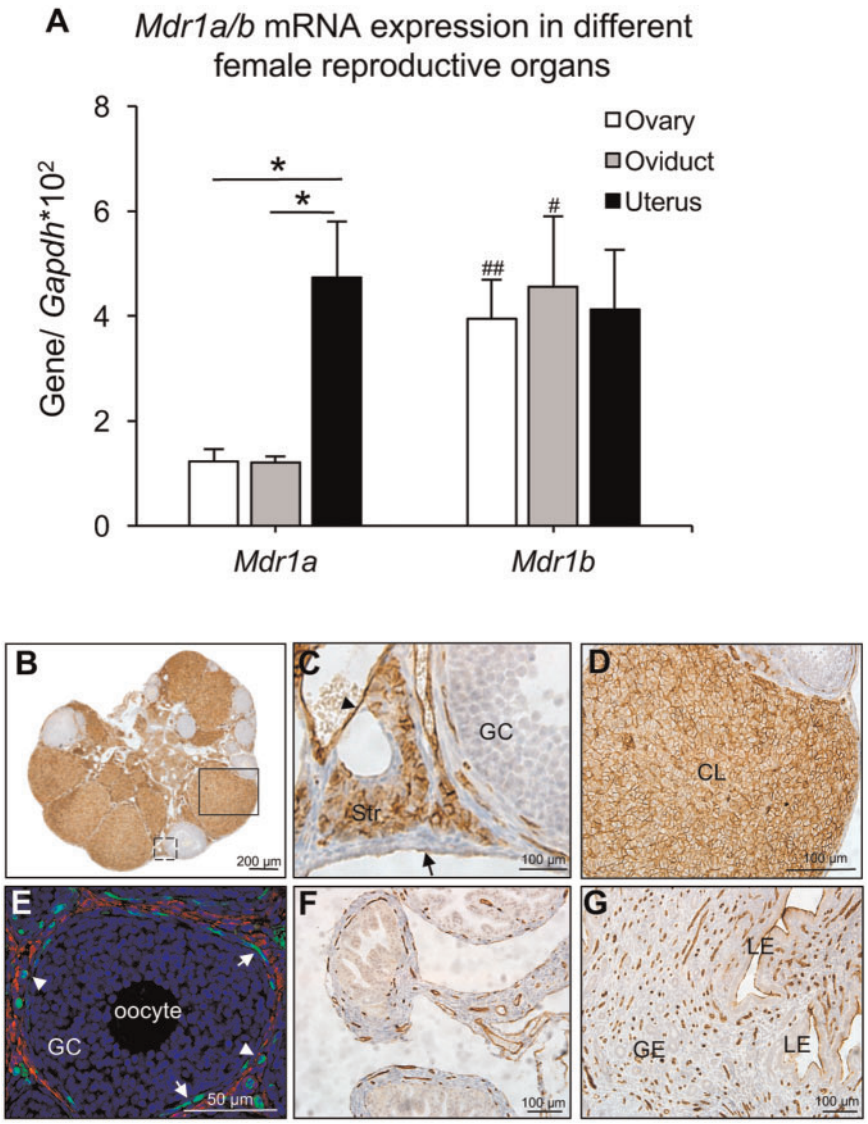

Figure 1. The expression of MDR1 in the female reproductive system. A, mRNA expression levels of *Mdr1a* and *Mdr1b* examined by RT-qPCR. $^{*}p < .05$ for the expression of *Mdr1a* in the uterus compared with that in the ovary and oviduct, $^{\#}p < .05$ and $^{\#\#}p < .01$ for the expression of *Mdr1b* compared with *Mdr1a* in the oviduct and ovary, respectively. Error bar: SD. Expression of MDR1 (brown staining) examined by IHC in the whole ovary (B), ovarian epithelial, stromal, and endothelial cell (C, black dash square in B), and CL (D, black square in B). E, IF staining of MDR1 (green) and α-SMA (red) in theca cell layers. IHC staining of MDR1 in the oviduct (F) and uterus (G). Arrow head and arrow in C indicated the endothelial cells of blood vessel and ovarian epithelial cells, respectively; arrow in E indicated the interna theca cells and the arrow head in E indicated the blood vessels in theca cell layers. Scale bar: 200 μm in B, 100 μm in C, D, F, G, and 50 μm in E. Str, stroma; CL, corpus luteum; GC, granulosa cells; LE, luminal epithelium; GE, glandular epithelium. Blue staining in E: DAPI ($n = 4$–5 female mice for each reproductive tissue and 3–5 replicates of IHC and IF staining were performed).

showed similar expression levels in all 3 examined organs (Figure 1A) . When compared with *Mdr1b*, the *Mdr1a* had significantly lower expression levels in the ovary and oviduct but the 2 isoforms had comparable expression levels in the uterus (Figure 1A). These results suggest that *Mdr1b* is the major isoform in the ovary and oviduct and the uterus has similar amount of both 2 isoforms.

Because the isoform-specific antibodies are not commercially available, the rabbit antiMDR1 antibody used for IHC and IF recognized both MDR1a and MDR1b. The kidney was used as positive control and results indicated that MDR1 was highly expressed in the renal tubule cells (Supplementary Figure 1A). In the ovary, MDR1 is expressed in the epithelial cells, stroma cells, endothelial cells of blood vessels, thecal cell layers, and luteal cells in the ovary (Figs. 1B–D). MDR1 showed similar expression pattern in the prepubertal ovary except that there was no CL (Supplementary Figure 1C); in the adult ovaries at different stages of estrous cycle, there were also similar expression patterns except that MDR1 had higher expression levels in the mature CL but had lower expression levels in the newly formed and degenerated CL, which will be discussed later. In the theca cell layers, the co-staining of MDR1 and α-SMA indicated that MDR1 was detectable in the interna theca cells and endothelial cells of blood vessels but not in the externa smooth muscle cells (Figure 1E). In the oviduct, MDR1 was only observed in the endothelial cells of the blood vessels in the stroma and smooth muscle cell layers (Figure 1F); in the uterus, MDR1 was expressed in the apical side of uterine luminal epithelium and the endothelial cells of blood vessels (Figure 1G). These results demonstrate that MDR1 is expressed in the female reproductive system and

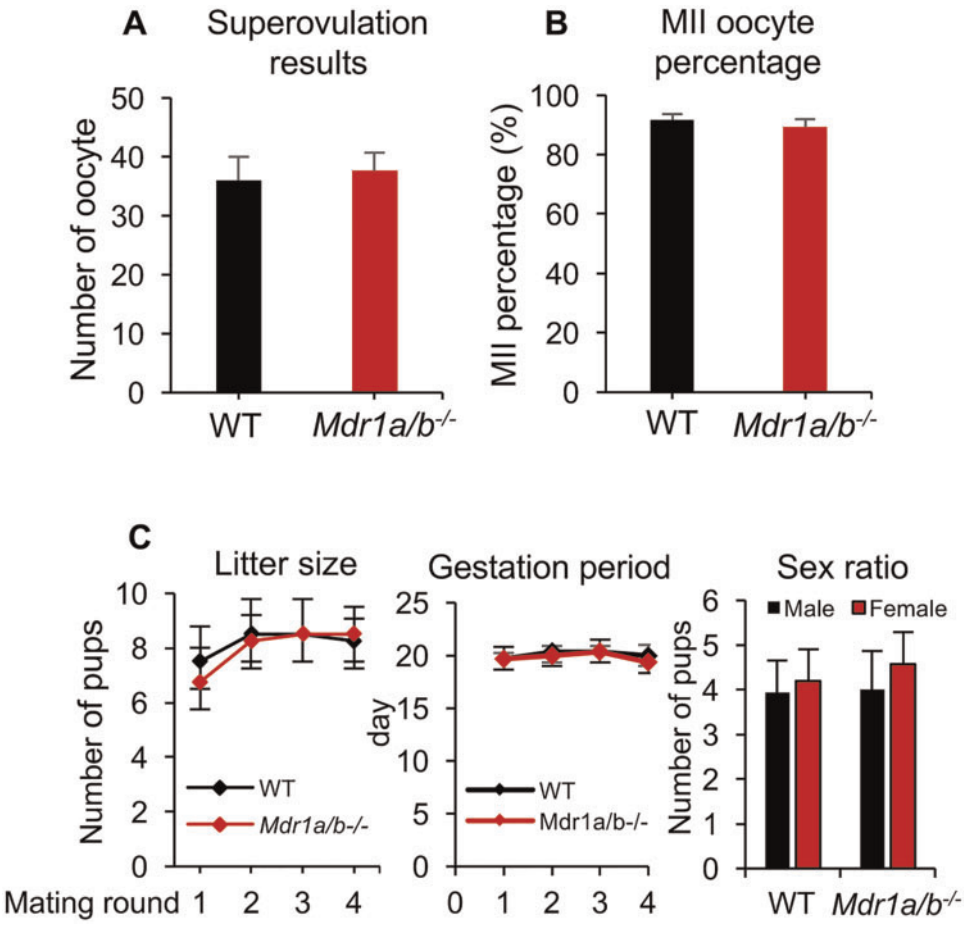

Figure 2. Effect of MDR1 deficiency on female mouse ovarian function and fertility. The number of superovulated oocytes collected from oviduct (A) and the MII percentage of these oocytes (B) in WT and *Mdr1a/b*$^{-/-}$ female mice. C, The average number of litter size, gestation period, and sex ratio for 4 mating rounds in WT and *Mdr1a/b*$^{-/-}$ female mice. Error bar: SD ($n = 4$–6 female mice for each experiment and 3 replicates were performed).

has various expression patterns in different female reproductive organs. Since the primary objective of this study was to determine the role of MDR1 in protecting the ovary from chemotherapy-induced damage, we next focused on the functions of MDR1 in the ovary in the following experiments.

The Lack of MDR1 Did Not Affect Female Mouse Ovarian Function and Fertility

To determine whether the MDR1 deficiency affects female ovarian function and fertility, histology, superovulation, and fertility test were performed in both WT and *Mdr1a/b*$^{-/-}$ mice. Histology results revealed similar ovarian morphology between WT and *Mdr1a/b*$^{-/-}$ genotypes in both prepubertal and adult mice (Supplementary Figure 2). Superovulation results indicated that there were comparable numbers of oocytes retrieved from oviduct between the 2 phenotypes of mice, with 36.0 ± 4.3 oocytes per WT mouse and 37.7 ± 3.1 oocyte per *Mdr1a/b*$^{-/-}$ mouse, respectively (Figure 2A). The percentage of oocytes had polar body extrusion and reached MII stage were also similar, with 91.2% ± 1.9% for WT mice and 90.4% ± 2.6% for *Mdr1a/b*$^{-/-}$ mice, respectively (Figure 2B). In fertility test, we counted the number of pups delivered by each mom for 4 mating rounds. Results indicated that the WT and *Mdr1a/b*$^{-/-}$ female mice had comparable litter size, gestation period, and sex ratio during the testing mating period (Figure 2C). Taken together these results demonstrate that the lack of MDR1 does not affect the examined ovarian reproductive outcomes and overall fertility.

The Lack of MDR1 Exacerbated DOX-Induced Ovarian Toxicity In Vivo

To determine whether the lack of MDR1 affects the susceptibility of female mice toward DOX-induced ovarian toxicity, WT and *Mdr1a/b*$^{-/-}$ female mice were treated with DOX at 0, 0.4, and 2 mg/kg body weight and various ovarian reproductive outcomes were assessed. TUNEL-staining results indicated that the DOX dose-dependently induced follicle apoptosis and the *Mdr1a/b*$^{-/-}$ ovaries had more apoptotic signals compared with WT ovaries treated with the same dosages of DOX (Figure 3A). To further examine the DOX-induced ovarian cell apoptosis in these 2 phenotypes, C-CASP3, a well-defined cell apoptotic marker, was quantified; and superovulation, a good indicator of follicle health and oocyte quality, was performed. Consistent with the TUNEL-staining results, DOX dose-dependently increased ovarian C-CASP3 levels and reduced the number of superovulated oocytes in WT mice (Figs. 3B and 3C in black color). When compared with WT mice with the same dosage of DOX exposure, the *Mdr1a/b*$^{-/-}$ mice with 0.4 mg/kg of DOX treatment had significantly decreased number of superovulated oocytes (Fig. 3B and 3C in red color); when the mice were treated with DOX at 2 mg/kg, both C-CASP3 levels and superovulation outcomes in *Mdr1a/b*$^{-/-}$ mice were more severely compromised

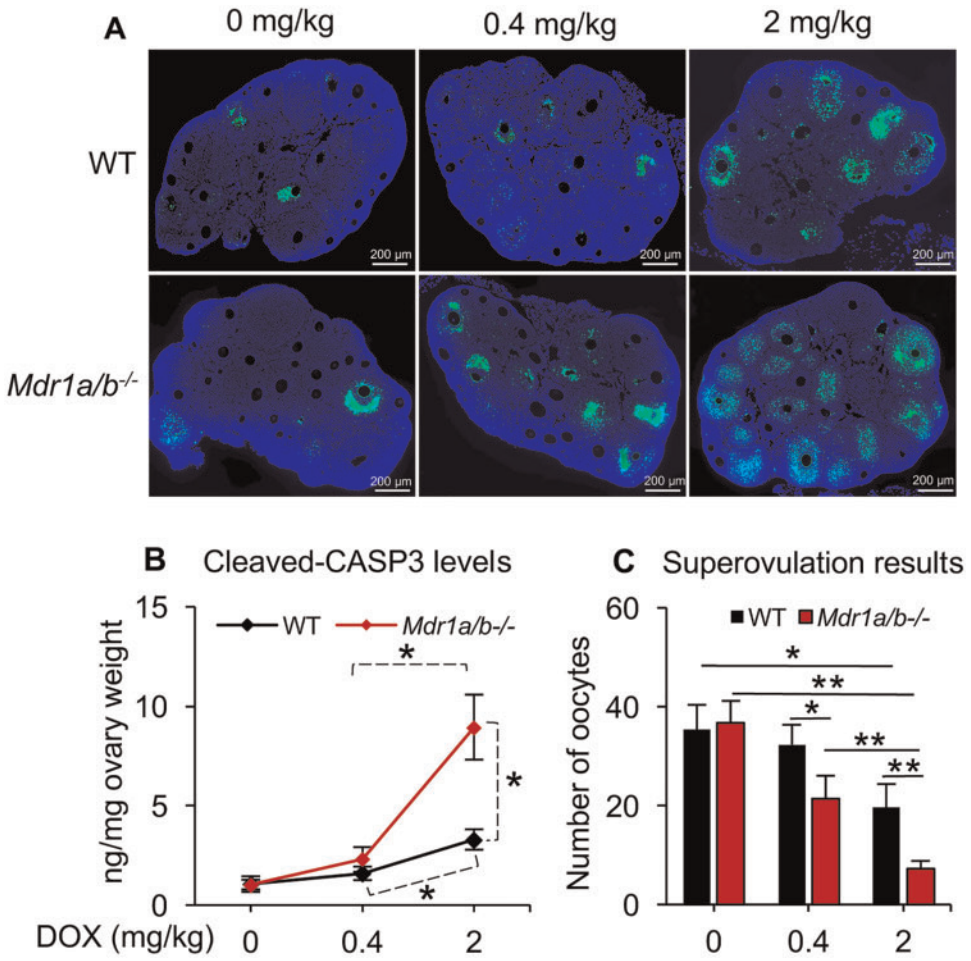

Figure 3. Effect of MDR1 deficiency on DOX-induced ovarian toxicity *in vivo*. A, Representative images of the ovaries with TUNEL staining upon 0, 0.4, and 2 mg/kg of DOX exposure *in vivo*. Blue, DAPI; green, apoptotic cells indicated by DNA fragmentation. Scale bar: 200 μm. B, C-CASP3 levels in the ovaries examined by ELISA. C, The number of superovulated oocyte in WT and *Mdr1a/b*$^{-/-}$ female mice upon 0, 0.4, and 2 mg/kg of DOX exposure *in vivo*. Error bar: SD; $^{*}p < .05$, $^{**}p < .01$ ($n = 4$–6 mice in each treatment group).

compared with those in WT mice (Figs. 3B and 3C in red color). These results indicate that the lack of MDR1 exacerbates DOX-induced ovarian toxicity.

Ovarian Follicles Exhibited MDR1-Mediated Efflux Activity

We next determined whether the MDR1 detected in ovarian cells exerts efflux activity and prevent the follicular cell influx and accumulation of its substrate, Rho123. Specifically, follicles were mechanically isolated, incubated with and without MDR1 inhibitor-PSC833, and stained with the MDR1 transported substrate-Rho123. As we detected the positive expression of MDR1 in stroma cell and theca cell layers, only follicles which displayed intact theca cell layers and with attached stroma cells were selected. In the follicles without MDR1 inhibitor treatment, the fluorescence intensity of Rho123 was gradually increased and the intensity in somatic cells was higher than that in oocytes (Figure 4A and black line in Figure 4B). Follicles treated with MDR1 inhibitor showed similar staining pattern, however, the green fluorescent intensity was significantly increased compared with follicles without inhibitor treatment at all the examined time points (10, 20, and 30 mins, respectively, Figure 4A and red line in Figure 4B), suggesting that the ovarian follicles could prevent the influx of Rho123 or pump Rho123 out of follicular cells which is mediated by MDR1.

The MDR1 Deficiency Exacerbated DOX-Induced Ovarian Toxicity In Vitro

The DOX exposure has been reported to result in a significantly reduced body weight and damages in other organs such as heart and liver in female mice (Desai *et al.*, 2013). Therefore, we next used the eIVFG method to determine whether the DOX-induced exacerbated ovarian toxicity in *Mdr1a/b*$^{-/-}$ mice is caused by the MDR1 deficiency in the ovary or requires the global MDR1 depletion and DOX-induced systemic toxicity. Both WT and *Mdr1a/b*$^{-/-}$ follicles were isolated, cultured, and exposed to different levels (0–100 nM) of DOX for analysis. Similar to the MDR1 efflux activity assay, only follicles which displayed intact theca cell layers and with attached stroma cells were selected. In both WT and *Mdr1a/b*$^{-/-}$ follicles without DOX treatment, the alginate encapsulation supported follicle growth from multilayered secondary stage to antral stage, with the follicle diameter increased from 167.7 ± 20.9 μm on day 0 to 320.7 ± 21.9 μm on day 8 for WT follicles and 159.0 ± 14.8 μm on day 0 to 319.1 ± 23.8 μm on day 8 for *Mdr1a/b*$^{-/-}$ follicles, respectively (Figs. 5A and 5B). The follicle survival rates on day 8 were also comparable when there was no DOX treatment (93.2% ± 8.0% and 92.9% ± 7.9 in WT and *Mdr1a/b*$^{-/-}$ follicles, respectively, Figs. 5C and 5D). These results confirm the *in vivo* results that the lack of MDR1 does not affect the ovarian function (Figure 2). Consistent

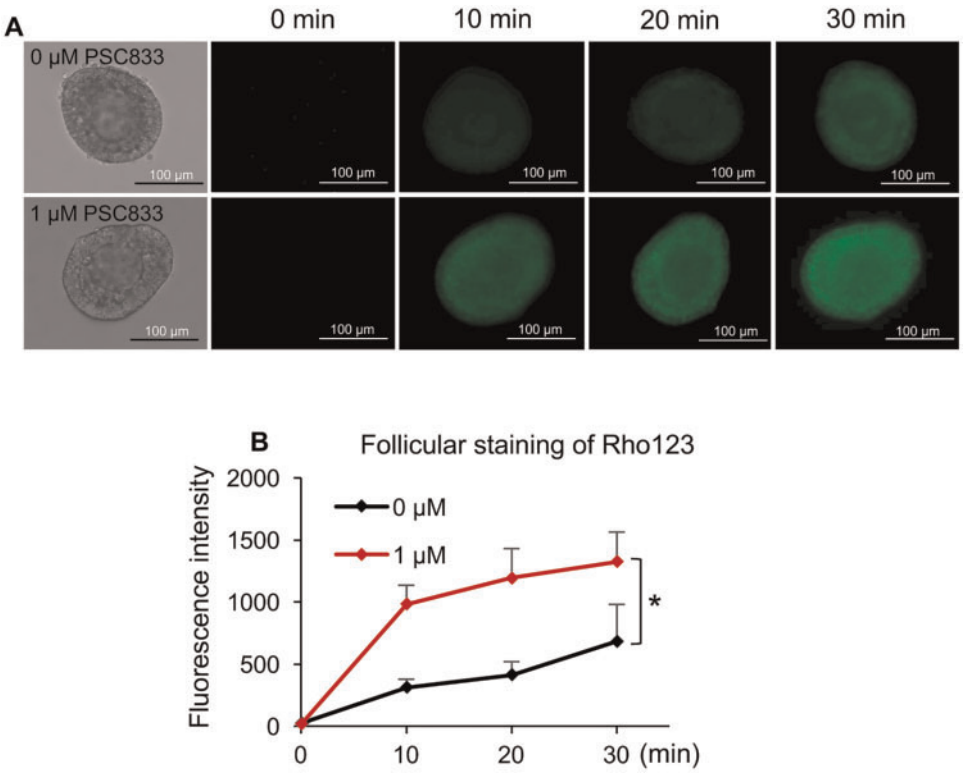

Figure 4. The MDR1-mediated efflux activity in ovarian follicles. A, Rho123 green fluorescence of representative follicles with and without MDR1 inhibitor PSC833 treatment. Scale bar: 100 μm. B, Quantification of Rho123 green fluorescence at different time with and without MDR1 inhibitor PSC833 treatment. Error bar: SD; $^{*}p < .05$ (n = 13–20 follicles for each treatment group and 3 replicates were included).

with our previous results (Xiao *et al.*, 2017), DOX at both 1 and 10 nM did not affect the WT follicle health but 100 nM of DOX significantly inhibited the follicle growth and decreased the follicle survival rate (Figs. 5A and 5C). In the *Mdr1a/b*$^{-/-}$ follicles treated with DOX at 1 nM, the follicle growth and survival rate were not significantly different from the WT follicles treated with DOX at 1 nM and *Mdr1a/b*$^{-/-}$ follicles without DOX treatment. However, when follicles were treated with DOX at 10 nM, the *Mdr1a/b*$^{-/-}$ follicle had significantly inhibited follicle growth and decreased survival rate compared with WT follicles with the same dosage of DOX treatment (Figure 5). Though 100 nM of DOX significantly affected the follicle growth and survival in both phenotypes of follicles, the *Mdr1a/b*$^{-/-}$ follicles exhibited significantly more severe damage patterns than the WT follicles, with survival rates at 23.85% VS 12.3% for WT and *Mdr1a/b*$^{-/-}$ follicles, respectively ($p = 0.013$, Figure 5). Furthermore, the LC50 of DOX on WT and *Mdr1a/b*$^{-/-}$ follicles was 68.4 nM (95% CI: 58.3–78.5 nM) and 12.7 nM (95% CI: 7.9–17.5 nM), respectively. These data demonstrate that the MDR1 deficiency in ovarian follicles promotes DOX-induced toxicity *in vitro* and the exacerbated DOX-induced ovarian toxicity in *Mdr1a/b*$^{-/-}$ mice does not require the MDR1 deletion in other non-ovarian tissues as well as the DOX-induced systemic toxicity.

The Expression of MDR1 in the Ovary Was Not Regulated by the Ovarian Steroid Hormones But Correlated to the Number and Status of CL

To characterize the hormonal regulation of MDR1 in the mouse ovary, RT-qPCR was performed to examine the expression of *Mdr1a* and *Mdr1b* in the ovaries at different stages of estrous cycle. Consistent with the results in Figure 1A, *Mdr1a* had much lower expression levels than *Mdr1b* (Figure 6A). *Mdr1a* and *Mdr1b* showed similar transcriptional patterns in the ovaries at different stages of estrous cycle with significantly higher expression levels at the estrus and metestrus stages than those at the proestrus and diestrus stages (Figure 6A). The serum concentrations of E2 and P4 were quantified by ELISA to further determine their influence on the MDR1 expression in the ovary. No significant associations were observed between the expression of both 2 MDR1 isoforms and the serum levels of E2 (top 2 figures of Figure 6B), and between the expression of *Mdr1a* and serum level of P4 (bottom left figure of Figure 6B). However, the expression of *Mdr1b* was positively correlated with the serum levels of P4 (with R^2 at 0.62, bottom right figure of Figure 6B), Moreover, we also found that the *Mdr1a* and *Mdr1b* mRNA levels were positively associated with the P4/E2 ratios (with R^2 at 0.56 and 0.77 for *Mdr1a* and *Mdr1b*, respectively, Figure 6C) which are indicator for the function of CL (Elgindy, 2011; Kamada *et al.*, 1992; Lee *et al.*, 2009).

To further examine the hormonal regulation of E2 and P4 on the expression of MDR1 in the ovary, ovarian explants with and without CL were treated with physiologically relevant levels of E2 and P4 *in vitro*, RT-qPCR results indicated that the ovarian explants with CL had comparable levels of *Mdr1a* and significantly higher levels of *Mdr1b* than the tissues without CL (Figure 7A). However, both E2 and P4 exposures did not change the expression of MDR1 in neither ovarian tissue with CL nor without CL (Figure 7A). These results suggest the changes of MDR1 expression in the ovary is not regulated by the ovarian steroid hormones but may be caused by the highly expressed MDR1 in luteal cells and the different number and status of CL at various stages of estrous cycle. To confirm this hypothesis,

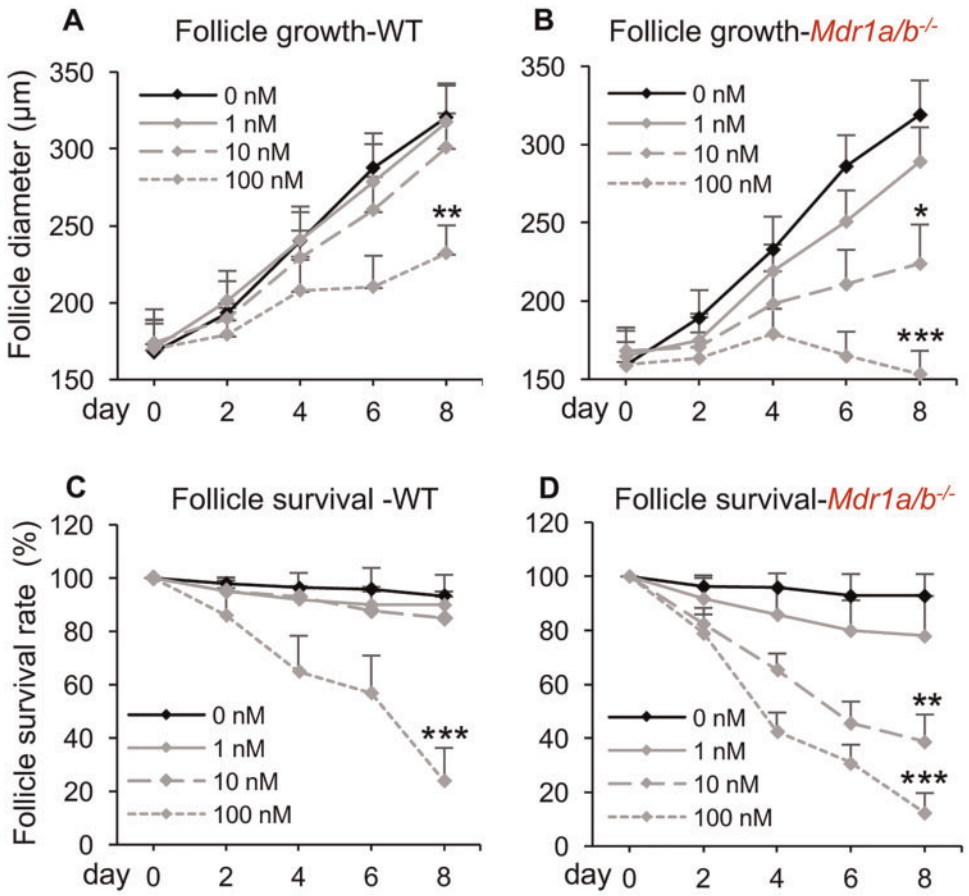

Figure 5. Effect of MDR1 deficiency on DOX-induced ovarian toxicity *in vitro*. Diameters of WT follicles (A) and *Mdr1a/b*$^{-/-}$ follicles (B) from days 0 to 8 after DOX exposure at 0–100 nM. Survival rates of WT follicles (C) and *Mdr1a/b*$^{-/-}$ follicles (D) from days 0 to 8 after DOX exposure at 0–100 nM. Error bar: SD; $^{*}p < .05$, $^{**}p < .01$, and $^{***}p < .001$ compared with the same genotype of follicles without DOX exposure ($n = 12$–15 follicles for 3 replicates).

IHC was performed to examine the expression of MDR1 in the ovaries at different stages of estrous cycle. Results indicated that MDR1 had similar expression levels in the stromal cells and theca cell layers at all stages of estrous cycle, however, it was highly expressed in the mature CL but was significantly lower in the newly formed and degenerated CL (Figure 7B). We also quantified the various status of CL in the ovaries at different stages of estrous cycle. Consistent with both RT-qPCR and IHC results (Figs. 6A and 7B), the expression levels of MDR1 in the ovary was not correlated to the total number of CL but had the same pattern with the average number of mature CL at different stages of estrous cycle (Figure 7C, R^2=0.82). Taken together, these results demonstrate that the different expression levels of MDR1 in the ovary is caused by the dynamic number and status of CL at different stages of estrous cycle.

DISCUSSION

MDR1, one of the most important efflux membrane transporter is expressed in both cancerous cells and normal tissues. In cancerous cells, although the underlying mechanism is not entirely understood, the overexpression of MDR1 is believed to be one of the major reasons to cause multidrug resistance during chemotherapies. Specifically, MDR1 functions as an efflux pump by exporting substrates from intracellular to extracellular compartment of the cell plasma membrane, which results in the lack of enough intracellular drug concentrations to kill tumorous cells (Takara *et al.*, 2006). In normal tissues, MDR1 functions to protect these tissues/cells from toxic compound accumulation and their subsequent toxicities (Amin, 2013; Fojo *et al.*, 1987). In the current study, we demonstrate that MDR1 is positively expressed in the female reproductive system including the ovary, oviduct, and uterus and the lack of MDR1 does not affect female fertility but promotes the DOX-induced ovarian toxicity.

The physiological function of MDR1 was first discovered by Schinkel *et al.* (1994) who detected the positive expression of MDR1 in the endothelial cells of the capillaries of blood-brain barrier. Moreover, MDR1 has also been detected in the hepatocytes in the liver, epithelial cells of small intestines and renal tubules of kidney, and syncytiotrophoblast of placenta (Sun *et al.*, 2006; Thiebaut *et al.*, 1987). Our study showed that MDR1 was expressed in the epithelial cells, theca cell layers, stroma cells, luteal cells, and endothelial cells in the ovary. However, there was no MDR1 detected in the oocytes and granulosa cells in the ovaries at all stages of estrous cycle (Figs. 1 and 7). These results are consistent with the findings in a study that examined the MDR1 in human female reproductive tissues (Finstad *et al.*, 1990), but are different from other studies which reported the positive expression of MDR1 in oocyte and granulosa cells (Arai *et al.*, 2006; Brayboy *et al.*, 2013, 2017; Fukuda *et al.*, 2006). With respect to the oocyte, one possible reason could be the species difference because the previous studies examined MDR1 in porcine and human oocytes but we use the mouse model (Arai *et al.*, 2006; Brayboy *et al.*, 2013). For the granulosa

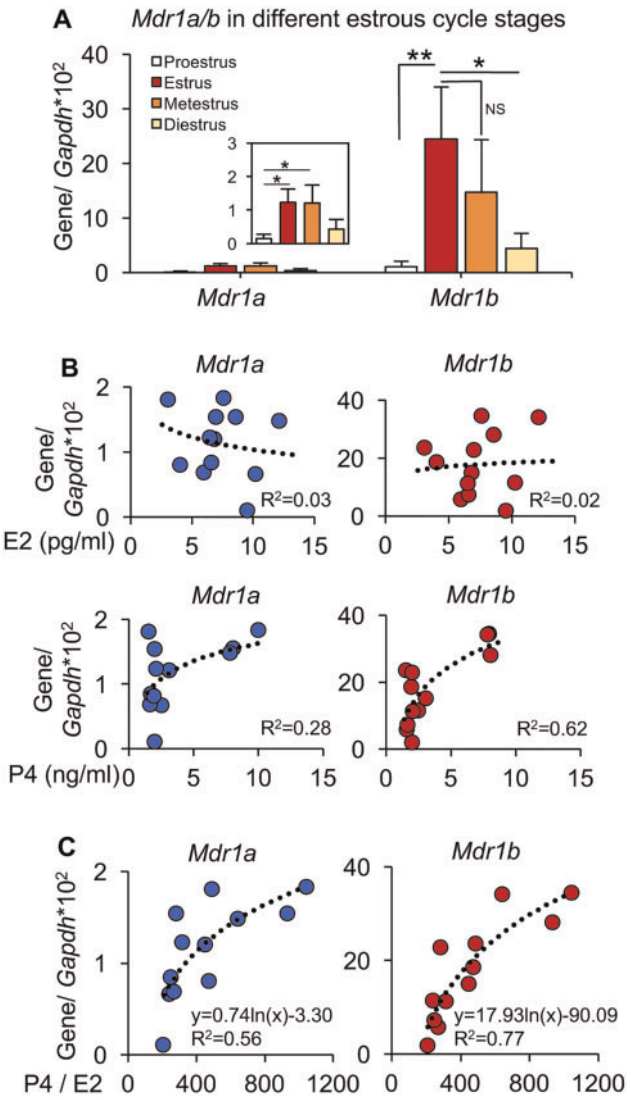

Figure 6. Association between the ovarian steroid hormone secretion and MDR1 expression in the ovary. A, The mRNA expression levels of *Mdr1a* and *Mdr1b* in the ovaries at different stages of estrous cycle. Error bar: SD; $^{*}p < .05$, $^{**}p < .01$, and NS, non-significant. The correlations between the mRNA expression levels of *Mdr1a* and *Mdr1b* in the ovaries and the corresponding serum concentrations of E2 and P4 (B) and P4/E2 ratios (C). R^2, coefficient of determination. Error bar: SD ($n = 3$–5 mice for each estrous cycle stage).

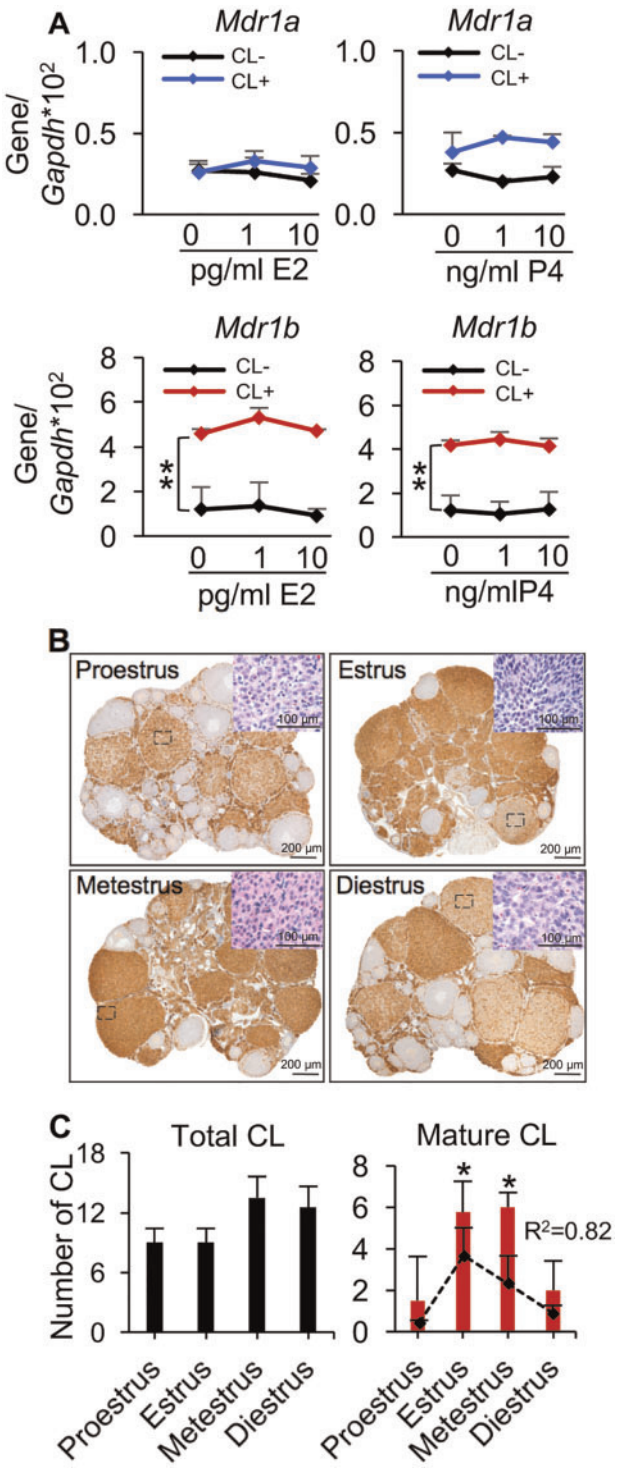

Figure 7. Association between the MDR1 expression in the ovary and CL. A, The mRNA expression levels of *Mdr1a* and *Mdr1b* in the ovaries with and without CL upon different concentrations of E2 and P4 treatments *in vitro*. B, Representative images of MDR1 expression examined by IHC (brown staining) in the ovaries at different stages of estrous cycle; the inserted H&E-stained images indicated the representative degenerated CL at proestrus and diestrus stages, newly formed CL at estrus stage, and mature CL metestrus stage. Scare bar: 200 μm for the images with IHC staining and 100 μm for the inserted H&E-stained images. C, The total number of CL (left) and average number of mature of CL (right) at different stages of estrous cycle. The black dash line indicated the corresponding expression of *Mdr1b*. CL−, ovaries without CL; CL+, ovaries with CL; R^2, coefficient of determination. Error bar: SD; $^{*}p < .05$; $^{**}p < .01$ ($n = 3$–5 mice for each estrous cycle stage).

cells, consistent with the results from a previous study (Brayboy *et al.*, 2017), we also find that MDR1 is highly expressed in the luteal cells and stroma cells (Figure 1). However, we didn't detect any positive MDR1 signals in the granulosa cells from both prepubertal ovary and ovaries at all stages of estrous cycle (Figs. 1 and 7, and Supplementary Figure 1C). Moreover, Salih *et al.* found that the overexpression of MDR1 attenuated the DOX-induced cytotoxicity in KK15 immortalized murine granulosa cells *in vitro* (Salih, 2011). In their study, the expression of MDR1 in these granulosa cells were not naturally expressed but induced by the retrovirus-mediated transfection method. Furthermore, it is also possible that the *in vitro* cultured granulosa cells are luteinized because it has been previously reported that the immortalized granulosa cells expressed higher levels of luteinizing hormone receptor and produced more P4, suggesting that the granulosa cells were transformed to luteal cells to some extent (Briers *et al.*, 1993; Vanderstichele *et al.*, 1994).

Considering the high levels of MDR1 in the luteal cells (Figs. 1 and 7), we expect that the positive expression of MDR1 in cultured granulosa cells may be caused by the granulosa cell luteinization. However, it is not clear why MDR1 is activated when granulosa cells are differentiated to luteal cells and further studies are needed.

The theca cell layers are believed to originate from ovarian stroma cells and are present in growing follicles (Young and McNeilly, 2010). Our results demonstrate that the presence of MDR1 in cells surrounding various stages of follicles is consistent with the dynamic development of theca cell layers and only the follicles with 2 or more layers of granulosa cells have positive signals (Figure 1). Theca cell layers contain various cell types including the interna theca cells, blood vessels, and externa smooth muscle cell layers (Fraser and Duncan, 2009). The co-staining of MDR1 and α-SMA indicate that the MDR1 is expressed in both interna theca cells and endothelial cells of blood vessels but not in externa smooth muscle cells. It is believed that the expression of MDR1 in noncancerous cells functions to restrict the accumulation of toxic chemicals as well as to protect these tissues from chemical-induced toxicity (Thiebaut *et al.*, 1987). Here, we expect the similar function of MDR1 in the ovary. For example, the major function of interna theca cells is to secret androgens which can be further converted to estrone and E2 by granulosa cells and the blood vessels embedded in theca cell layers are responsible for providing nutrients and other factors to support follicle maturation (Young and McNeilly, 2010), suggesting that the MDR1 expressed in the theca cell layers may exert the protective functions to maintain the normal ovarian steroidogenesis and follicle maturation. In addition to the ovary, we also found the positive expression of MDR1 in the endothelial cells of oviduct and luminal epithelial cells and endothelial cells in the uterus (Figure 1). The expression and function of MDR1 in the oviduct and nonpregnant uterus was rarely studied, but the positive signals of MDR1 may also suggest the protective functions in these 2 organs.

MDR1 can recognize a broad range of structurally diverse compounds and more than 50 MDR1 substrates have been reported (Hodges *et al.*, 2011). Here, we selected DOX, a validated MDR1 substrate as well as a confirmed ovarian toxic chemical (Dantzig *et al.*, 1996; Luker *et al.*, 2001), to determine the role of MDR1 in protecting against chemotherapy-induced ovarian toxicity. The dosage of DOX used for anticancer treatments ranges from 0.1 to 10 mg/kg which depends on the cancer type, disease progression, and patients' body size (Ferguson *et al.*, 1993; Scheithauer *et al.*, 1985). After entering systemic circulation, the plasma concentration of DOX is maintained at 2–100 nM for 20–30 h and with DOX but not its metabolite-doxorubicinol as the primary cytotoxic chemical (Speth *et al.*, 1988; Sturgill *et al.*, 2000). It has also been reported that 2–10 mg/kg of DOX significantly increased mouse ovarian follicle apoptosis and oocyte degeneration and reduced the ovulation rate and litter size *in vivo* (Ben-Aharon *et al.*, 2010; Kropp *et al.*, 2015; Roti Roti *et al.*, 2012; Xiao *et al.*, 2017), and the DOX has dose-dependent toxicity on cultured follicles with LC50 at 75.5 nM *in vitro* (Xiao *et al.*, 2017). Therefore, in the current study, the human relevant exposure levels of DOX at 0–2 mg/kg and 0–100 nM were selected for *in vivo* and *in vitro* experiments, respectively, to assess whether the lack of MDR1 exacerbate the DOX-induced ovarian toxicity.

In the *in vivo* experiments, the results of superovulation, oocyte meiotic division, and fertility test in nonchemotherapy treated mice demonstrate that the lack of MDR1 does not impact both ovarian function and overall fertility in female mice (Figure 2). However, the DOX dose-dependently increased the ovarian follicle apoptosis and decreased the number of superovulated oocytes in WT mice and these reproductive outcomes were further compromised in the female mice with MDR1 deficiency, indicating the protective functions of MDR1 on the DOX-induced ovarian cell damages (Figure 3). Since the DOX exhibits adverse impacts in multiple organs such as liver and heart, we further performed the *in vitro* studies to differentiate the local impacts from the systemic impacts. The Rho123 fluorescence-staining assay confirms that the MDR1 expressed in the stroma cells and thecal cell layers exhibit MDR1-mediated drug efflux activity (Figure 4). Furthermore, the *in vitro* DOX exposure experiments demonstrate that the lack of MDR1 makes follicles more susceptible to the DOX-induced ovarian toxicity and this adverse impact does not require the global MDR1 deficiency as well as the systemic toxicity from DOX exposure (Figure 5).

The ovarian hormonal regulation of MDR1 has been reported in a few studies, however, the results are still controversial (Coles *et al.*, 2009; Fukuda *et al.*, 2006; Mutoh *et al.*, 2006b). Coles *et al.* (2009) found that both E2 and P4 upregulated the MDR1 expression in the JAR placental cells, while another study showed the E2 downregulated and P4 did not impact the MDR1 expression in human breast cancer cells, MCF-7 (Mutoh *et al.*, 2006b). In cultured porcine granulosa cells, results from Fukuda *et al.* (2006) showed that P4 increased MDR1 expression but E2 had no effect. These inconsistent results could be caused by different cell types and different hormone exposure strategies used in these studies. Consistent with recently published data (Brayboy *et al.*, 2017), we also found that mice have the highest *Mdr1a/b* expression levels in the estrus and metestrus stages. However, after comparing the individual serum E2 or P4 concentrations and the *Mdr1a* or *Mdr1b* expression levels in the ovaries, no significant correlation was observed, but the expression of both MDR1 isoforms are positively correlated with the P4/E2 ratios (Figure 6). P4/E2 ratio is widely used as a biomarker to indicate the function of CL and to predict the success of *in vitro* fertilization and pregnancy (Elgindy, 2011; Kamada *et al.*, 1992; Lee *et al.*, 2009). We therefore hypothesize that the dynamic changes of MDR1 expression maybe caused by the changed CL at different stages of estrous cycle. Our *in vitro* E2 and P4 exposure experiments confirm that the MDR1 expression is significantly increased in the ovaries with CL compared with the ovaries without CL; the ovarian expression of MDR1 is not regulated by E2 or P4 treatment but correlated with the numbers and status of corpora lutea (Figure 7). However, since the ovarian explants with and without CL were collected from 16 to 26 days old mice, respectively, we cannot exclude the potential influence of age on the ovarian expression of MDR1 and more studies are necessary. It is not well understood why MDR1 is negative in the granulosa cells but activated and highly expressed in luteal cells, but we expect that it may exert the protective functions to maintain the normal progesterone secretion in the CL and prevent the progesterone insufficiency from xenobiotic exposure, which are critical for the successful establishment of uterine receptivity and embryo implantation (El Zowalaty *et al.*, 2017; Wang and Dey, 2006).

As the essential roles of MDR1 in inducing the multidrug resistance during chemotherapy, MDR1 inhibitors are currently investigated to overcome the MDR1-mediated efflux activities and to improve the anticancer drug delivery. For example, the third-generation of MDR1 inhibitors including tariquidar and zosuquidar have been tested in phase III clinical trials to determine whether they could prolong the efficacy of chemotherapeutics (Roe *et al.*, 1999; Starling *et al.*, 1997). However, these

MDR1 inhibitors also compromise the MDR1 functions in normal tissues and subsequently increase the chemotherapy-induced side effects (Wessler *et al.*, 2013). Furthermore, several human MDR1 genetic variants including the nonfunctional single nucleotide polymorphism have been discovered to affect the MDR1 efflux activity (Leschziner *et al.*, 2007; Mutoh *et al.*, 2006a; Sai *et al.*, 2003), which will also change the susceptibility of these people to the chemotherapy-induced side effects. With respect to the female reproductive system, the ovarian failure and infertility would be the major concerns among young female cancer patients because both the inactivation and inhibition of MDR1's efflux activity will promote the chemotherapy-induced ovarian toxicity and infertility. In conclusion, our study demonstrates that the lack of MDR1 promotes DOX-induced ovarian toxicity, suggesting the critical role of MDR1 in protecting female ovarian functions during chemotherapy.

SUPPLEMENTARY DATA

Supplementary data are available at *Toxicological Sciences* online.

Funding

Arnold School of Public Health Start Up Fund to S.X. and Magellan Scholar Program to S.X. and M.K. in the University of South Carolina and National Institute of Environmental Health Science NIEHS at NIH (1UG3ES029073-01); Center for Reproductive Health After Disease from the National Institutes of Health National Center for Translational Research in Reproduction and Infertility (NCTRI) (P50HD076188) to J.Z.

ACKNOWLEDGMENT

We thank Dr Teresa K. Woodruff in Northwestern University for the helpful suggestions on the initiation of this project and experimental design.

REFERENCES

Abraham, J., Edgerly, M., Wilson, R., Chen, C., Rutt, A., Bakke, S., Robey, R., Dwyer, A., Goldspiel, B., and Balis, F. (2009). A phase I study of the P-glycoprotein antagonist tariquidar in combination with vinorelbine. *Clin. Cancer Res.* **15**, 3574–3582.

Altenberg, G. A., Vanoye, C. G., Horton, J. K., and Reuss, L. (1994). Unidirectional fluxes of rhodamine 123 in multidrug-resistant cells: Evidence against direct drug extrusion from the plasma membrane. *Proc. Natl. Acad. Sci. U.S.A.* **91**, 4654–4657.

Amin, M. L. (2013). P-glycoprotein inhibition for optimal drug delivery. *Drug Target Insights* **7**, 27–34.

Arai, M., Yamauchi, N., Fukuda, H., Soh, T., and Hattori, M. A. (2006). Development of multidrug resistance type I P-glycoprotein function during in vitro maturation of porcine oocyte. *Reprod. Toxicol.* **21**, 34–41.

Arceci, R. J., Croop, J. M., Horwitz, S. B., and Housman, D. (1988). The gene encoding multidrug resistance is induced and expressed at high-levels during pregnancy in the secretory epithelium of the uterus. *Proc. Natl. Acad. Sci. U.S.A.* **85**, 4350–4354.

Bar-Joseph, H., Ben-Aharon, I., Rizel, S., Stemmer, S. M., Tzabari, M., and Shalgi, R. (2010). Doxorubicin-induced apoptosis in germinal vesicle (GV) oocytes. *Reprod. Toxicol.* **30**, 566–572.

Ben-Aharon, I., Bar-Joseph, H., Tzarfaty, G., Kuchinsky, L., Rizel, S., Stemmer, S. M., and Shalgi, R. (2010). Doxorubicin-induced ovarian toxicity. *Reprod. Biol. Endocrinol.* **8**, 20.

Bines, J., Oleske, D. M., and Cobleigh, M. A. (1996). Ovarian function in premenopausal women treated with adjuvant chemotherapy for breast cancer. *J. Clin. Oncol.* **14**, 1718–1729.

Borst, P., and Schinkel, A. H. (2013). P-glycoprotein ABCB1: A major player in drug handling by mammals. *J. Clin. Investig.* **123**, 4131–4133.

Brayboy, L. M., Oulhen, N., Long, S., Voigt, N., Raker, C., and Wessel, G. M. (2017). Multidrug resistance transporter-1 and breast cancer resistance protein protect against ovarian toxicity, and are essential in ovarian physiology. *Reprod. Toxicol.* **69**, 121–131.

Brayboy, L. M., Oulhen, N., Witmyer, J., Robins, J., Carson, S., and Wessel, G. M. (2013). Multidrug-resistant transport activity protects oocytes from chemotherapeutic agents and changes during oocyte maturation. *Fertil. Steril.* **100**, 1428–1435.

Briers, T. W., van de Voorde, A., and Vanderstichele, H. (1993). Characterization of immortalized mouse granulosa cell lines. *In Vitro Cell Dev. Biol. Anim.* **29**, 847–854.

Byers, S. L., Wiles, M. V., Dunn, S. L., and Taft, R. A. (2012). Mouse estrous cycle identification tool and images. *PLoS One* **7**, e35538.

Chabner, B. A., and Roberts, T. G. Jr. (2005). Timeline: Chemotherapy and the war on cancer. *Nat. Rev. Cancer* **5**, 65–72.

Coles, L. D., Lee, I. J., Voulalas, P. J., and Eddington, N. D. (2009). Estradiol and progesterone-mediated regulation of P-gp in P-gp overexpressing cells (NCI-ADR-RES) and placental cells (JAR). *Mol. Pharm.* **6**, 1816–1825.

Cordon-Cardo, C., O'Brien, J. P., Casals, D., Rittman-Grauer, L., Biedler, J. L., Melamed, M. R., and Bertino, J. R. (1989). Multidrug-resistance gene (p-glycoprotein) is expressed by endothelial-cells at blood-brain barrier sites. *Proc. Natl. Acad. Sci. U.S.A.* **86**, 695–698.

Dantzig, A. H., Shepard, R. L., Cao, J., Law, K. L., Ehlhardt, W. J., Baughman, T. M., Bumol, T. F., and Starling, J. J. (1996). Reversal of P-glycoprotein-mediated multidrug resistance by a potent cyclopropyldibenzosuberane modulator, LY335979. *Cancer Res.* **56**, 4171–4179.

Desai, V. G., Herman, E. H., Moland, C. L., Branham, W. S., Lewis, S. M., Davis, K. J., George, N. I., Lee, T., Kerr, S., and Fuscoe, J. C. (2013). Development of doxorubicin-induced chronic cardiotoxicity in the B6C3F1 mouse model. *Toxicol. Appl. Pharmacol.* **266**, 109–121.

El Zowalaty, A. E., Li, R., Zheng, Y., Lydon, J. P., DeMayo, F. J., and Ye, X. (2017). Deletion of rhoA in progesterone receptor-expressing cells leads to luteal insufficiency and infertility in female mice. *Endocrinology* **158**, 2168–2178.

Elgindy, E. A. (2011). Progesterone level and progesterone/estradiol ratio on the day of hCG administration: Detrimental cutoff levels and new treatment strategy. *Fertil. Steril.* **95**, 1639–1644.

Ferguson, J. E., Dodwell, D. J., Seymour, A. M., Richards, M. A., and Howell, A. (1993). High dose, dose-intensive chemotherapy with doxorubicin and cyclophosphamide for the treatment of advanced breast cancer. *Br. J. Cancer* **67**, 825–829.

Finstad, C. L., Saigo, P. E., Rubin, S. C., Federici, M. G., Provencher, D. M., Hoskins, W. J., Lewis, J. L., Jr., and Lloyd, K. O. (1990). Immunohistochemical localization of P-glycoprotein in adult human ovary and female genital tract of patients with benign gynecological conditions. *J. Histochem. Cytochem.* **38**, 1677–1681.

Fojo, A. T., Ueda, K., Slamon, D. J., Poplack, D. G., Gottesman, M. M., and Pastan, I. (1987). Expression of a multidrug-resistance gene in human tumors and tissues. *Proc. Natl. Acad. Sci. U.S.A.* **84**, 265–269.

Forster, S., Thumser, A. E., Hood, S. R., and Plant, N. (2012). Characterization of rhodamine-123 as a tracer dye for use in in vitro drug transport assays. *Plos One* **7**, e33253.

Fraser, H. M., and Duncan, W. C. (2009). SRB reproduction, fertility and development award lecture 2008. Regulation and manipulation of angiogenesis in the ovary and endometrium. *Reprod. Fertil. Dev.* **21**, 377–392.

Fukuda, H., Arai, M., Soh, T., Yamauchi, N., and Hattori, M. A. (2006). Progesterone regulation of the expression and function of multidrug resistance type I in porcine granulosa cells. *Reprod. Toxicol.* **22**, 62–68.

Gottesman, M. M., and Pastan, I. (1988). The multidrug transporter, a double-edged sword. *J. Biol. Chem.* **263**, 12163–12166.

Hodges, L. M., Markova, S. M., Chinn, L. W., Gow, J. M., Kroetz, D. L., Klein, T. E., and Altman, R. B. (2011). Very important pharmacogene summary: aBCB1 (MDR1, P-glycoprotein). *Pharmacogenet. Genomics* **21**, 152–161.

Huang, Q. T., Shynlova, O., Kibschull, M., Zhong, M., Yu, Y. H., Matthews, S. G., and Lye, S. J. (2016). P-glycoprotein expression and localization in the rat uterus throughout gestation and labor. *Reproduction* **152**, 195–204.

Kalabis, G. M., Kostaki, A., Andrews, M. H., Petropoulos, S., Gibb, W., and Matthews, S. G. (2005). Multidrug resistance phosphoglycoprotein (ABCB1) in the mouse placenta: Fetal protection. *Biol. Reprod.* **73**, 591–597.

Kamada, S., Kubota, T., and Aso, T. (1992). Influence of progesterone/estradiol ratio on luteal function for achieving pregnancy in gonadotropin therapy. *Horm. Res.* **37**, 59–63.

Kartner, N., Evernden-Porelle, D., Bradley, G., and Ling, V. (1985). Detection of P-glycoprotein in multidrug-resistant cell lines by monoclonal antibodies. *Nature* **316**, 820–823.

Kolitz, J. E., George, S. L., Marcucci, G., Vij, R., Powell, B. L., Allen, S. L., DeAngelo, D. J., Shea, T. C., Stock, W., Baer, M. R., *et al.* (2010). P-glycoprotein inhibition using valspodar (PSC-833) does not improve outcomes for patients younger than age 60 years with newly diagnosed acute myeloid leukemia: Cancer and Leukemia Group B study 19808. *Blood* **116**, 1413–1421.

Kropp, J., Roti Roti, E. C., Ringelstetter, A., Khatib, H., Abbott, D. H., and Salih, S. M. (2015). Dexrazoxane diminishes doxorubicin-induced acute ovarian damage and preserves ovarian function and fecundity in mice. *PLoS One* **10**, e0142588.

Lankas, G. R., Wise, L. D., Cartwright, M. E., Pippert, T., and Umbenhauer, D. R. (1998). Placental P-glycoprotein deficiency enhances susceptibility to chemically induced birth defects in mice. *Reprod. Toxicol.* **12**, 457–463.

Lee, F. K., Lai, T. H., Lin, T. K., Horng, S. G., and Chen, S. C. (2009). Relationship of progesterone/estradiol ratio on day of hCG administration and pregnancy outcomes in high responders undergoing in vitro fertilization. *Fertil. Steril.* **92**, 1284–1289.

Lee, J. S., Paull, K., Alvarez, M., Hose, C., Monks, A., Grever, M., Fojo, A. T., and Bates, S. E. (1994). Rhodamine efflux patterns predict P-glycoprotein substrates in the National Cancer Institute drug screen. *Mol. Pharmacol.* **46**, 627–638.

Leschziner, G. D., Andrew, T., Pirmohamed, M., and Johnson, M. R. (2007). ABCB1 genotype and PGP expression, function and therapeutic drug response: A critical review and recommendations for future research. *Pharmacogenomics J.* **7**, 154–179.

Luker, G. D., Flagg, T. P., Sha, Q., Luker, K. E., Pica, C. M., Nichols, C. G., and Piwnica-Worms, D. (2001). MDR1 P-glycoprotein reduces influx of substrates without affecting membrane potential. *J. Biol. Chem.* **276**, 49053–49060.

Morgan, S., Anderson, R. A., Gourley, C., Wallace, W. H., and Spears, N. (2012). How do chemotherapeutic agents damage the ovary? *Hum. Reprod. Update* **18**, 525–535.

Mutoh, K., Mitsuhashi, J., Kimura, Y., Tsukahara, S., Ishikawa, E., Sai, K., Ozawa, S., Sawada, J., Ueda, K., Katayama, K., *et al.* (2006a). A T3587G germ-line mutation of the MDR1 gene encodes a nonfunctional P-glycoprotein. *Mol. Cancer Ther.* **5**, 877–884.

Mutoh, K., Tsukahara, S., Mitsuhashi, J., Katayama, K., and Sugimoto, Y. (2006b). Estrogen-mediated post transcriptional down-regulation of P-glycoprotein in MDR1-transduced human breast cancer cells. *Cancer Sci.* **97**, 1198–1204.

Perez, G. I., Knudson, C. M., Leykin, L., Korsmeyer, S. J., and Tilly, J. L. (1997). Apoptosis-associated signaling pathways are required for chemotherapy-mediated female germ cell destruction. *Nat. Med.* **3**, 1228–1232.

Riordan, J. R., Deuchars, K., Kartner, N., Alon, N., Trent, J., and Ling, V. (1985). Amplification of P-glycoprotein genes in multidrug-resistant mammalian cell lines. *Nature* **316**, 817–819.

Roe, M., Folkes, A., Ashworth, P., Brumwell, J., Chima, L., Hunjan, S., Pretswell, I., Dangerfield, W., Ryder, H., and Charlton, P. (1999). Reversal of P-glycoprotein mediated multidrug resistance by novel anthranilamide derivatives. *Bioorg. Med. Chem. Lett.* **9**, 595–600.

Roti Roti, E. C., Leisman, S. K., Abbott, D. H., and Salih, S. M. (2012). Acute doxorubicin insult in the mouse ovary is cell- and follicle-type dependent. *PloS One* **7**, e42293.

Sai, K., Kaniwa, N., Itoda, M., Saito, Y., Hasegawa, R., Komamura, K., Ueno, K., Kamakura, S., Kitakaze, M., Shirao, K., *et al.* (2003). Haplotype analysis of ABCB1/MDR1 blocks in a Japanese population reveals genotype-dependent renal clearance of irinotecan. *Pharmacogenetics* **13**, 741–757.

Salih, S. M. (2011). Retrovirus-mediated multidrug resistance gene (MDR1) overexpression inhibits chemotherapy-induced toxicity of granulosa cells. *Fertil. Steril.* **95**, 1390–1396 e1-6.

Scheithauer, W., Zielinksi, C., and Ludwig, H. (1985). Weekly low dose doxorubicin monotherapy in metastatic breast cancer resistant to previous hormonal and cytostatic treatment. *Breast Cancer Res. Treat.* **6**, 89–93.

Schinkel, A. H., Smit, J. J., van Tellingen, O., Beijnen, J. H., Wagenaar, E., van Deemter, L., Mol, C. A., van der Valk, M. A., Robanus-Maandag, E. C., te Riele, H. P., *et al.* (1994). Disruption of the mouse mdr1a P-glycoprotein gene leads to a deficiency in the blood-brain barrier and to increased sensitivity to drugs. *Cell* **77**, 491–502.

Speth, P. A., van Hoesel, Q. G., and Haanen, C. (1988). Clinical pharmacokinetics of doxorubicin. *Clin. Pharmacokinet.* **15**, 15–31.

Starling, J. J., Shepard, R. L., Cao, J., Law, K. L., Norman, B. H., Kroin, J. S., Ehlhardt, W. J., Baughman, T. M., Winter, M. A., Bell, M. G., *et al.* (1997). Pharmacological characterization of LY335979: A potent cyclopropyldibenzosuberane modulator of P-glycoprotein. *Adv. Enzyme Regul.* **37**, 335–347.

Stocco, C., Telleria, C., and Gibori, G. (2007). The molecular control of corpus luteum formation, function, and regression. *Endocr. Rev.* **28**, 117–149.

Sturgill, M. G., August, D. A., and Brenner, D. E. (2000). Hepatic enzyme induction with phenobarbital and doxorubicin metabolism and myelotoxicity in the rabbit. *Cancer Investig.* **18**, 197–205.

Sun, M., Kingdom, J., Baczyk, D., Lye, S. J., Matthews, S. G., and Gibb, W. (2006). Expression of the multidrug resistance P-glycoprotein, (ABCB1 glycoprotein) in the human placenta decreases with advancing gestation. *Placenta* **27**, 602–609.

Takara, K., Sakaeda, T., and Okumura, K. (2006). An update on overcoming MDR1-mediated multidrug resistance in cancer chemotherapy. *Curr. Pharm. Des.* **12**, 273–286.

Thiebaut, F., Tsuruo, T., Hamada, H., Gottesman, M. M., Pastan, I., and Willingham, M. C. (1987). Cellular localization of the multidrug-resistance gene product P-glycoprotein in normal human tissues. *Proc. Natl. Acad. Sci. U.S.A.* **84**, 7735–7738.

Vanderstichele, H., Delaey, B., de Winter, J., de Jong, F., Rombauts, L., Verhoeven, G., Dello, C., van de Voorde, A., and Briers, T. (1994). Secretion of steroids, growth factors, and cytokines by immortalized mouse granulosa cell lines. *Biol. Reprod.* **50**, 1190–1202.

Wang, H., and Dey, S. K. (2006). Roadmap to embryo implantation: Clues from mouse models. *Nat. Rev. Genet.* **7**, 185–199.

Wessler, J. D., Grip, L. T., Mendell, J., and Giugliano, R. P. (2013). The P-glycoprotein transport system and cardiovascular drugs. *J. Am. Coll. Cardiol.* **61**, 2495–2502.

Xiao, S., Duncan, F. E., Bai, L., Nguyen, C. T., Shea, L. D., and Woodruff, T. K. (2015). Size-specific follicle selection improves mouse oocyte reproductive outcomes. *Reproduction* **150**, 183–192.

Xiao, S., Zhang, J., Liu, M., Iwahata, H., Rogers, H. B., and Woodruff, T. K. (2017). Doxorubicin has dose-dependent toxicity on mouse ovarian follicle development, hormone secretion, and oocyte maturation. *Toxicol. Sci.* **157**, 320–329.

Young, J. M., and McNeilly, A. S. (2010). Theca: The forgotten cell of the ovarian follicle. *Reproduction* **140**, 489–504.

Zhao, F., Li, R., Xiao, S., Diao, H. L., Viveiros, M. M., Song, X., and Ye, X. Q. (2013). Postweaning exposure to dietary zearalenone, a mycotoxin, promotes premature onset of puberty and disrupts early pregnancy events in female mice. *Toxicol. Sci.* **132**, 431–442.